

# Kinetic Study of Oxygen Reduction Reaction on Palladium Nanoparticles Supported in Thermally Treated Carbon

R. Gonzalez Huerta<sup>1,\*</sup>, P. Gonzalez Puente<sup>1</sup> and O. Solorza Feria<sup>2</sup>

<sup>1</sup>Instituto Politécnico Nacional, IPN-ESIQIE, Laboratorio de Electroquímica y Corrosión, UPALM, Ed. 8, 07830, México D.F. México

<sup>2</sup>Depto. Química, Centro de Investigación y de Estudios Avanzados del IPN, A. Postal 14-740, 07360 México, D.F.

Received: November 04, 2010, Accepted: January 22, 2011, Available online: April 07, 2011

**Abstract:** The kinetic study of oxygen reduction reaction (ORR) using palladium nanoparticles supported in thermally-treated Vulcan<sup>®</sup> carbon as an electrocatalyst was developed in a 0.5 M H<sub>2</sub>SO<sub>4</sub> solution. The Vulcan<sup>®</sup> carbon was thermally treated at 400°C and 600°C. The Pd supported in thermally treated carbon (Pd/TTC) was synthesized by PdCl<sub>2</sub> reduction with NaBH<sub>4</sub> in water at 60°C. The thermally treated carbon (TTC) was evaluated by Raman spectroscopy, whereas the morphology of Pd/TTC was characterized by Scanning Electron Microscopy (SEM). The electrochemical activity was studied by rotating disk electrode (RDE) and rotating ring-disk electrode (RRDE) techniques. The RDE result showed a high activity of the Pd/TTC towards the ORR, this reaction proceeds preferentially via a 4e<sup>-</sup> pathway. On the other hand, the hydrogen peroxide productions were 4.6% and 6.6% for Pd/TTC at 400°C and 600°C, respectively.

**Keywords:** Electrocatalyst, Pd compounds, hydrogen peroxide, PEMFC.

## 1. INTRODUCTION

Proton exchange membrane fuel cells (PEMFC) present themselves as power sources for vehicles, portable devices and stationary applications. However, their commercialization is still limited by several issues, including poor kinetic and high overpotentials associated with oxygen reduction reaction ORR [1]. In PEMFC, the low interaction between the electrocatalyst and the support has been the subject of intensive research in recent years. Electrochemical corrosion of carbon in the potential operational range of fuel cell causes aggregation/dissolution of nanocatalysts and is certainly one important factor that contributes to reducing the performance and durability of fuel cells. This corrosion concurrently increases surface hydrophobicity, influencing the gas transport in electrodes [2-5]. Therefore, it is important to develop novel supports for fuel cell systems. Vulcan XC-72<sup>®</sup> carbon black with a high surface area is the most used substrate support due to its electric conductivity and chemical stability in acidic media.

In order to improve the electrochemical performance of nanometric-sized Pd in the present research, the palladium was

supported in thermally treated carbon (TTC at 400°C and 600°C) synthesized by the reduction of the transition metal chlorides with NaBH<sub>4</sub> [6-9]. Rotating disk electrode (RDE) and rotating ring-disk electrode (RRDE) techniques were employed to evaluate the kinetics and selectivity towards the ORR and to elucidate the electric transfer pathway reaction.

## 2. EXPERIMENTAL

### 2.1. Electrocatalyst Preparation

Nanometric Pd/TTC catalyst has been synthesized by a NaBH<sub>4</sub> reduction of PdCl<sub>2</sub> in 50 ml H<sub>2</sub>O, following the methodology reported in the literature [7-11]. Carbon thermal treatment (Vulcan carbon XC-72<sup>®</sup>) was done in order to activate a number of superficial groups to favor the interaction with the palladium catalyst and also to eliminate the possibility of its containing impurities. Carbon powder was weighed (400mg) in a quartz container and subjected to thermal treatment in an air atmosphere at 400°C and 600°C, in a temperature-controlled Lindberg furnace at 10°C/min for 1 hour. Thereafter, the resultant powder was maintained in a closed vessel inside a desiccator. Palladium nanoparticles were synthesized by mixing 35 mg of PdCl<sub>2</sub> and 180 mg of thermally treated carbon (TTC) in a Pyrex<sup>®</sup> chemical reactor containing 50

\*To whom correspondence should be addressed:  
Email: rosgonzalez\_h@yahoo.com.mx  
Phone: 57296000, ext. 55392

ml of water at 60°C. After vigorous agitation, a homogeneous mixture was obtained. Then 50 mg of NaBH<sub>4</sub> was added, maintaining the agitation of the solution for 2 hours. Afterwards, the reaction product was washed several times to eliminate the produced sodium chloride, and the powder was filtered and kept in a closed vessel. The reaction time and experimental conditions were enough to produce nanometric catalysts, obtaining a 99% yield.

## 2.2. Physical Characterization

Raman spectroscopy has been widely used to study and characterize the different forms of carbon [12,13]. In the case of Vulcan carbon especially, this technique has been very successful in providing information as to structural properties; carbon cannot be tested by conventional infrared analysis because the spectra have the same behavior. The structural properties of TTC were identified by Raman spectroscopy and carried out with a Raman Station 400F PerkinElmer, operating at a scanned range from 1000 cm<sup>-1</sup> to 1900 cm<sup>-1</sup>, with laser power at 80%. The spectra were recorded with a spectral slit width of 2 cm<sup>-1</sup>, with an exposition time of 3 seconds and 3 expositions [7]. Particle size and morphology of Pd/TTC powders were determined from scanning electron microscopy analysis (SEM), with a Sirion XL30 FEG-SEM-FEI microscope, operating at 5 kV.

## 2.3. Electrochemical Characterization

All electrochemical measurements were carried out at 25°C in a single, conventional, three-electrode test electrochemical cell in a 0.5M H<sub>2</sub>SO<sub>4</sub> aqueous solution. A platinum mesh was used as the counter electrode, and Hg/Hg<sub>2</sub>SO<sub>4</sub>/0.5M H<sub>2</sub>SO<sub>4</sub> (MSE=0.680 V/NHE) as the reference electrode. Experiments were performed in a Potentiostat AutoLab and a Pine MSR-X rotation speed controller. The potentials in this paper were related to normal hydrogen electrode (NHE).

Rotating disk electrode (RDE) and rotating ring-disk electrode (RRDE) techniques were employed for the purpose of determining the main reaction pathway and the amount of hydrogen peroxide produced during the oxygen reduction reaction. For RDE experiments, 8 μl of a sonicated mixture of 1mg of catalyst, 60 μl of ethyl alcohol (spectrum grade), and 6 μl of 5wt% solution Nafion® (Du Pont, 1000EW) were deposited on glassy carbon electrode (GC) with a cross-sectional area of 0.19 cm<sup>2</sup>. The estimated amount of catalyst on the GC surface was about 0.63 mg cm<sup>-2</sup>. For RRDE, a commercial RRDE-PAR glassy carbon disk (diam=5 mm), and platinum ring with 0.22 of nominal collection efficiency [14,15] was employed as a working electrode. The catalytic ink was prepared with 1mg of catalyst, 8 μl of 5 wt% solution Nafion® (Du Pont, 1100 EW), 100 μl of water, and 100 μl of ethyl alcohol (spectrum grade). 8 μl of this suspension were deposited on the working electrode. The estimated amount of catalyst on the electrode surface was about 0.20 mg cm<sup>-2</sup>.

Before the ORR measurements, cyclic voltammetry (CV) was performed from 0.05 to 1.25 V at 50 mV s<sup>-1</sup> in a nitrogen-saturated electrolyte, to clean the electrode surface. Forty cycles were necessary to stabilize the current-potential signal. Thereafter, the acid electrolyte was saturated with pure oxygen and maintained on the electrolyte surface during the RDE and RRDE tests. Hydrodynamic experiments were recorded in the rotation rate range of 100 to 2500 rpm at 5 mV s<sup>-1</sup>. Between RDE and RRDE measurements, the acid

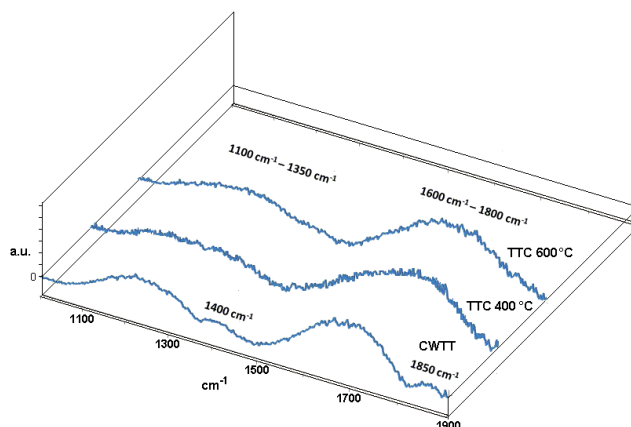


Figure 1. Raman spectra of thermal treated carbon at 400°C and 600°C.

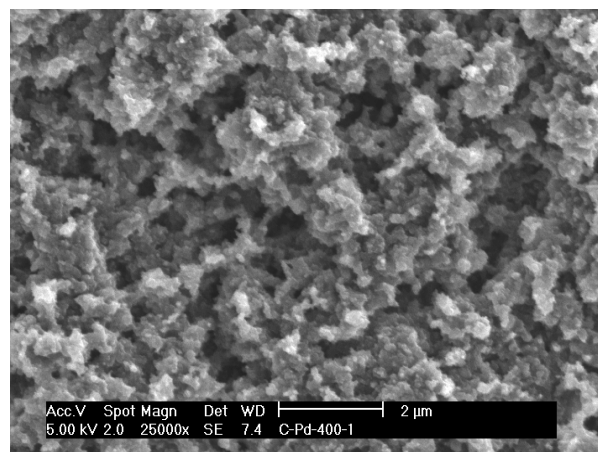


Figure 2. SEM image of palladium catalyst thermally treated at 400°C.

electrolyte was saturated with pure oxygen for 5 minutes to obtain the stable open circuit potential. The current density was calculated using the geometric surface area.

## 3. RESULTS AND DISCUSSION

### 3.1. Physical Characterization

The support substrate plays an important role on catalysts, i.e., enhancing dispersion of the catalyst, preventing aggregation; reducing the required loading of the catalyst; and improving catalytic activity as a co-catalyst. The Vulcan carbon XC-72® is a popular substrate used to support nanoparticles. It has high surface area, electric conductivity, and chemical stability - but many times the carbon has impurities, mainly sulphur compounds [16].

The Raman spectra are shown in Figure 1, including carbon without thermal treatment (CWTT). The CWTT and the TTC at 400 and 600°C spectra show two prominent bands, between the 1100 cm<sup>-1</sup>-1350 cm<sup>-1</sup> and 1600 cm<sup>-1</sup>-1800 cm<sup>-1</sup> ranges, attributed to the presence of C-O and C=O groups respectively. This is characteristic of amorphous carbon. However, two relatively small bands

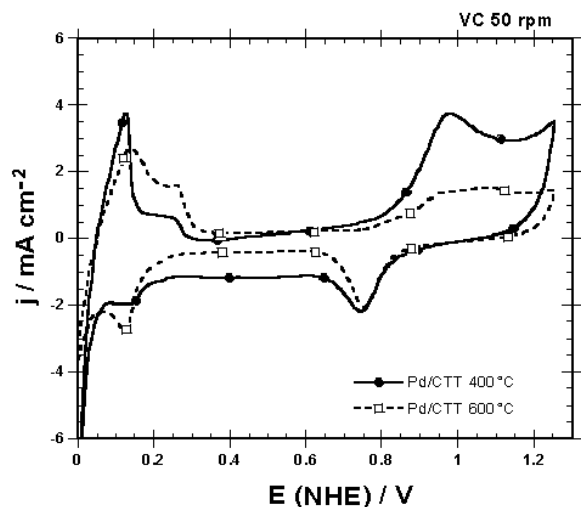


Figure 3. Cyclic voltammograms of palladium electrodes in a de-gassed 0.5M H<sub>2</sub>SO<sub>4</sub> electrolyte. The potential was scanned at 50 mV s<sup>-1</sup>.

at 1400 cm<sup>-1</sup> and 1850 cm<sup>-1</sup>, associated with the impurities, are present in the CWTT. The TTC does not show these bands, thus the thermal treatment removed the carbon impurities [7].

SEM image of the powder catalyst with thermally treated carbon at 400°C is shown in Figure 2. SEM analysis of the palladium powder morphology showed a rough surface with irregular spherical agglomerates embedded in an amorphous phase, among the sizes from 50 to 100 nm; the other thermally treated sample shows a similar morphology.

### 3.2. Electrochemical results

The cyclic voltammetry (CV) characterization of the palladium electrode in the supporting electrolyte was performed in a nitrogen-purged 0.5 M H<sub>2</sub>SO<sub>4</sub> solution, at a 50mV s<sup>-1</sup> scan rate. In this experiment, the electrodes were submitted to 40 cycles in order to obtain reproducible voltammograms. Figure 3 presents voltammograms of the two palladium samples for comparison purposes. The supported palladium electrodes present voltammograms with defined peaks associated with adsorption/desorption hydrogen, which are characteristics in polycrystalline noble metals. The voltammogram of the palladium electrodes with thermally treated carbon shows similar surface reactions in a potential region of 0.0 V–0.35 V/NHE. Analysis at a more positive potential, corresponding to the anodic region, also shows a well-defined hydroxide-adsorbed peak with a striking difference in the current magnitude, which indicates that a Pd/(TTC at 400°C) shows a better capacity for anion adsorption compared to Pd/(TTC at 600°C). Cathodic scan shows a slight difference in the current magnitude of the oxide reduction.

Figure 4 shows RDE experiments. The polarization curves on palladium supported in thermally treated carbon at 400 °C, incorporated into a Nafion® film electrode, were performed at different rotation rates, in an oxygen-saturated 0.5M H<sub>2</sub>SO<sub>4</sub> solution at 25°C. The polarization curves show three well defined potential zones: charge transfer, mixed and mass transport. It was considered that defined limiting currents are associated with the high diffusion of

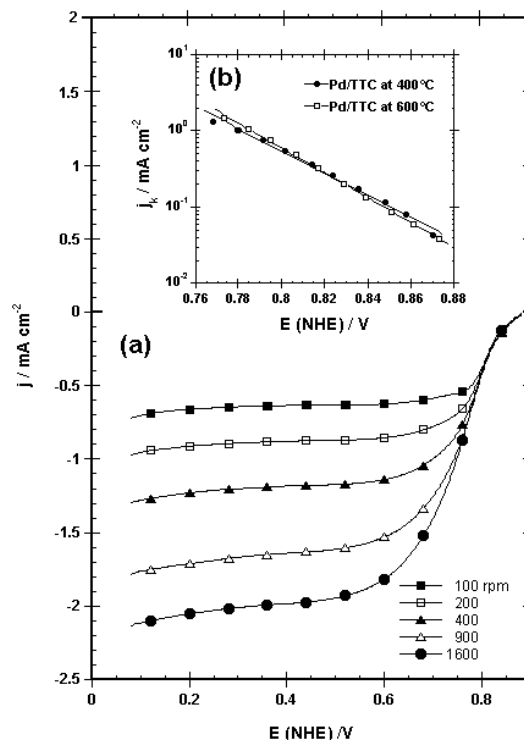


Figure 4. RDE responses on supporting Pd/TTC electrodes in O<sub>2</sub> saturated 0.5 M H<sub>2</sub>SO<sub>4</sub>: a) Linear Voltammetry, b) Tafel plot.

oxygen through the electrode surface and the uniform distribution of active sites. A similar polarization curve was observed on the Pd/(TTC at 600°C) electrode. In these electrocatalysts, the oxygen reduction is fast enough that, at high overpotentials, a flat limiting plateau is observed [17]. This phenomenon can be associated to a good distribution of the electrocatalytic sites on the electrode surfaces.

On a film-coated electrode surface, the overall measured density current ( $i$ ), is related to the kinetic density current ( $i_k$ ), the boundary layer-layer diffusion-limited density current ( $i_d$ ), and the film diffusion-limited current ( $i_f$ ), by equation (1). The effect of the film diffusion is significant only in cases where the electrode is covered by the Nafion film and can be neglected in the present study since the amount of Nafion (1 $\mu$ l 5 wt.% Nafion in 11  $\mu$ l of solution) in the prepared catalyst suspension is sufficiently small. Hence, it should not be considered a factor in the limiting current density [9,18]. Thus, the overall measured current of the oxygen reduction can be written as being dependent on the kinetic current and the diffusion-limited current, as shown on the left side of the following equation:

$$\frac{1}{i} = \frac{1}{i_k} + \frac{1}{i_L} + \frac{1}{i_f} = \frac{1}{i_k} + \frac{1}{B\omega^{1/2}} \quad (1)$$

The kinetic current density is proportional to the intrinsic activity of the catalyst. The constant  $B$  is  $0.2nFCD^{2/3}v^{-1/6}$   $0.2nF$ , where 0.2 is a constant used when  $\omega$  is expressed in revolutions per minute,  $C$  is the bulk concentration of oxygen ( $1.1 \times 10^{-6}$  mol cm<sup>-3</sup>),  $D$  is the

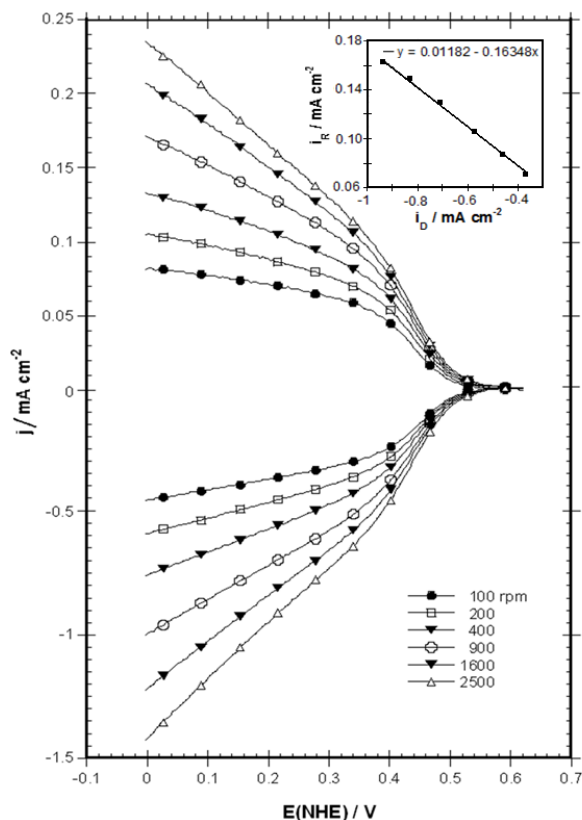


Figure 5. RRDE polarization curves: a) Polarization curves disk-ring electrode using  $5 \times 10^{-3}$  M  $\text{K}_3\text{Fe}(\text{CN})_6$  solution in 0.1 M  $\text{K}_2\text{SO}_4$  at different rotation speeds and b) The collection efficiency ( $N$ ) from the slope of an  $i_R$  versus  $i_D$  plot

diffusion coefficient of oxygen in the sulfuric acid solution ( $1.4 \times 10^{-5} \text{ cm}^2 \text{ s}^{-1}$ ), and  $\nu$  is the kinematic viscosity of the sulfuric acid ( $1.0 \times 10^{-2} \text{ cm}^2 \text{ s}^{-1}$ ) [9].

The inset in Figure 4 shows the mass-transfer-corrected Tafel plots for the Pd/(TTC at 400°C) and 600°C. Tafel slope at low current density has a value of  $70 \text{ mV dec}^{-1}$  and  $60 \text{ mVdec}^{-1}$  in the Pd/(TTC at 400°C) and 600°C respectively, which indicates that the first electron transfer on the adsorbed oxygen molecule is the rate-determining step. This behavior is in agreement with results reported by other authors for Pd and PdNi catalysts prepared by other synthetic methods [6-9].

The ORR is a complex reaction that proceeds via several consecutive and parallel elementary steps. It has been accepted that this occurs along two principal pathways: the first is the direct reduction to water with the transference of  $4e^-$ ; the second is the so-called “peroxide pathway”, which involves the transfer of  $2e^-$  to the formation of  $\text{H}_2\text{O}_2$  as intermediate [14]. In this study, the RRDE technique was used in order to determine the amount of hydrogen peroxide produced. The collection efficiency ( $N$ ) was obtained experimentally from the slope of an  $i_R$  versus  $i_D$  plot at different rotation speeds, using as an electrolyte a  $5 \times 10^{-3}$  M  $\text{K}_3\text{Fe}(\text{CN})_6$  solution in 0.1 M  $\text{K}_2\text{SO}_4$  (Figure 5). The inset in Figure 5 shows a value of  $N = 0.16$  for this arrangement. The ring potential was kept at

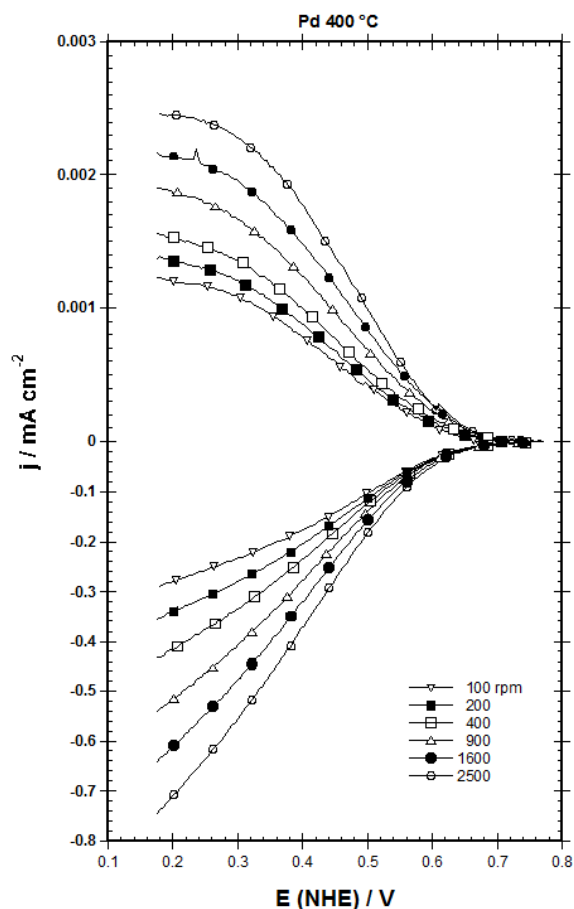


Figure 6. Steady-state polarization curves at different rotation speeds as a function of disk potentials for ORR in 0.5M  $\text{H}_2\text{SO}_4$ . Pd/TTC disk and Pt ring held at 1.48 V/NHE.

+1.48V (NHE) during all of the electrochemical experiments, where oxidation of the  $\text{H}_2\text{O}_2$  formed by  $\text{O}_2$  reduction on the disk electrode is limited by diffusion [14,15].

Steady-state polarization curves obtained for the ORR in the disk and the currents for the hydrogen peroxide oxidation in the ring to Pd/(TTC at 400 °C) electrode are shown in Figure 6. In the oxygen saturated solution, the diffusion currents in the disk and ring are observed as a function of rotation speed.

The disk currents ( $I_D$ ) do not reach a perfect plateau of the diffusion limited currents, this being due to the small amount of catalyst ( $0.20 \text{ mg cm}^{-2}$ ) on the thin film formed on the glassy carbon electrode with the catalytic ink. Nonetheless, it clearly defines its dependency on the rotating speed. The ring current ( $I_R$ ) in Figure 6 shows a dependence on the rotation rate and also does not reach a perfect plateau of the diffusion limited currents. The peroxide percentages were evaluated from the following equation [19]:

$$\% \text{H}_2\text{O}_2 = \frac{200 I_R / N}{I_D + I_R / N} \quad (2)$$

Figure 7 shows a potential dependence on the hydrogen peroxide

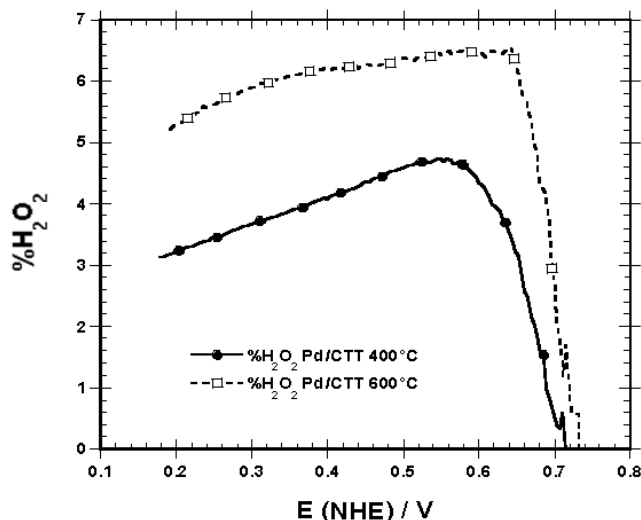


Figure 7. Percentage of H<sub>2</sub>O<sub>2</sub> produced from the molecular oxygen reduction on palladium supported in thermally treated carbon Pd/TTC at 400°C and 600°C.

formation. The amount of H<sub>2</sub>O<sub>2</sub> produced with the electrode potential in the electrochemical process of the ORR reaches a value of 6.5 % on Pd/(TTC at 600°C) electrode at 0.64 V/NHE, while on Pd/(TTC at 400°C) electrode it reaches a value of 4.7 % at 0.55 V/NHE. These results indicate that the Pd/TTC at 400 °C has a yield near 95.3 % for the ORR (i.e., %H<sub>2</sub>O = 100- %H<sub>2</sub>O<sub>2</sub>), following preferentially the four-electron transfer mechanisms to water formation (i.e., O<sub>2</sub>+4H<sup>+</sup>+4e<sup>-</sup>→2H<sub>2</sub>O) [15]. The best electrocatalyst is Pd/(TTC at 400°C) .

#### 4. CONCLUSION

A carbon black-supporting electrocatalyst was thermally treated at 400°C and 600°C to eliminate the impurities and favor the interaction between palladium and the support. The palladium powder morphology showed a rough surface with irregular spherical agglomerates embedded in an amorphous phase, with sizes from about 50 to 100 nm.

Well-defined polarization curves are associated with the high diffusion of oxygen through the electrode surface and the uniform distribution of active sites. A Tafel slope at a low current density of about 60 mV dec<sup>-1</sup> in the Pd/TTC catalysts indicates that the rate-determining step is the first electron transfer to the adsorbed oxygen molecule. The best electrocatalyst was Pd/TTC treated at 400 °C because it has a yield near 95.3 % for the ORR, following preferentially the four-electron transfer mechanisms to water formation. Additional efforts as to catalyst preparation should be carried out to reduce the amount of H<sub>2</sub>O<sub>2</sub> produced following this methodology.

#### 5. ACKNOWLEDGEMENTS

The authors gratefully acknowledge the financial support of IPN (project SIP-20100530) and ICYTDF (PICS08-37). The authors also wish to express their gratitude to Guadalupe Ramos for assistance in the catalytic synthesis and to Tim Godwin of

www.manuscriptex.com for the English-language editing.

#### REFERENCES

- [1] H.A. Gasteiger, S.S. Kocha, B. Sompalli, F.T. Wagner, Appl. Catal. B, 56, 9 (2005).
- [2] J. Oiao, B. Li and J. Ma, J. Electrochem. Soc. B, 436, 156 (2009).
- [3] A. Liu, Z. Brady, B. Carter, R. Litteer, B. Budinski, M. Hyun and J. Muller, J. Electrochem. Soc., 155, 979 (2008).
- [4] D. Santa Rosa, D. Pinto, V. Silva, R. Silva and C. Rangel, Int. J. Hydrogen Energy, 32, 4350 (2007).
- [5] C. Acharya, W. Li, Z. Liu, G. Kwon, C. Turner, A. Lane, D. Nikles, T. Klein, M. Weaver, J. Power Sources, 192, 324 (2009).
- [6] V. Collins, R. González, A. López, D. Delgado and O. Solorza, J. New Mat. Electrochem. Systems, 12, 63 (2009).
- [7] R.G. González, M. L. Luna, O. Solorza, ECS Transactions, 20, 267 (2009).
- [8] G. Ramos, H. Yee, O. Solorza, Inter. J. Hydrogen Energy, 33, 3596 (2008).
- [9] J. Salvador, S. Citalan, O. Solorza, J. Power Sources, 172, 229 (2007).
- [10] J. Prabhuram, T. Zhao, Z. Tang, R. Chen, Z. Liang, J. Phys. Chem. B, 110, 5245 (2006).
- [11] B. Veisz, L. Toth, D. Teschner, Z. Paal, N. Györfy, U. Wild, R. Schlogl, J. Mol. Catal. A: Chem., 238, 56 (2005).
- [12] J. Oiao, B. Li and J. Ma, J. Electrochem. Soc. B, 436, 156 (2009).
- [13] Ch. Castiglioni and M. Tommasini, Opt. Pura Apl., 40, 169 (2007).
- [14] K. Suarez, A. Rodríguez, S. Duron, O. Solorza, J. Power Sources, 171, 381 (2007).
- [15] G. Ramos, O. Solorza, J. Int. Hydrogen Energy, 35, 12105 (2010).
- [16] L. Timperman, Y.J. Feng, W. Vogel, N. Alonso, Electrochimica Acta, 55, 7558 (2010).
- [17] J. Murayama, I. Abe, Electrochimica Acta, 48, 1443 (2003).
- [18] V.S. Murthi, R.C. Urian, S. Mukerjee, J. Phys. Chem. B, 108, 11011 (2004).
- [19] U. Paulus, T. Schmidt, H. Gasteiger, R. Behm, J. Electroanalytic. Chem., 495, 134 (2001).